RAPID SOFT BED SLIDING OF THE PUGET GLACIAL LOBE

N. E. Brown, B. Hallet, and D. B. Booth

Quaternary Research Center and Department of Geological Sciences
University of Washington, Seattle

Abstract. The Puget lobe of the late Pleistocene Cordilleran ice sheet advanced into western Washington over a thick sequence of unlithified sediments. The basal drag due to sliding over this surface was calculated by (1) idealizing the sediment bed as a rigid planar surface scattered with roughness elements corresponding to individual sedimentary particles and (2) taking the minimum reconstructed sliding velocity to be 500 m yr^{-1}. The calculated basal drag, minimized by choices of parameters, is 400 kPa, much higher than the reconstructed gravitational driving stress of 40 kPa, indicating that a rigid bed and low water pressure are not consistent with the glacier's rapid motion. High subglacial water pressure, averaging 90% of the ice overburden (10 MPa) is inferred from overconsolidation of subglacial clays. The occurrence and deformation of water-deposited sediments within the till and the requirement to drain large quantities of water from the interface suggest that water pressure reached 99% of the ice overburden. Ploughing of till by ice-entrained clasts, pervasive shearing, and, finally, ice-bed separation become possible as water pressure increases. At the low inferred effective normal stress the basal drag is reduced from the rigid bed case by water layers which decouple the smallest particles from the glacier sole and ploughing which reduces the resistance offered by the largest particles. The limited shear strain observed in much of the till implies pervasive shearing did not contribute significantly to ice motion; basal motion was confined to the ice-bed interface or to distinct faults within the substrate.

Introduction

The Puget lobe of the Cordilleran ice sheet (in western North America) advanced southward into western Washington in the late Pleistocene, culminating roughly 14,500 years ago during the Vashon stade of the Fraser glaciation [Armstrong et al., 1965]. The Puget lobe was largely underlain by unlithified sediments (Figure 1). The considerable thickness of Vashon-age lodgment till, averaging 15 m in the Seattle area (based on well logs published by Liesch et al. [1963]) and of similar thickness throughout the lowland (Figure 2), implies that till rather than the underlying sediments constituted the bed of the Puget Lobe during most of the glacial occupation. The till is

inferred to be lodgment till based on the presence of oriented stones, oriented striations on stones, overconsolidation, and deformation features.

This paper investigates the rapid motion of the Puget lobe over its bed of deformable sediment. Studies of large, vanished glaciers complement basal motion studies of modern glaciers, in which the glacier geometry and velocity are well-constrained but the characteristics of the bed can only be inferred from observations over very limited areas [Kamb et al., 1985], seismic measurements [Blankenship et al., 1986] or modelling [Lingle and Brown, 1987]. Observations on glacier beds recently exposed by glacial retreat can provide information about conditions during a somewhat greater time span but are restricted to the marginal environment. In addition, inferences about the bed of modern glaciers are limited by the short duration and seasonality of the observations. A notable benefit of studying the beds of Pleistocene glaciers is that they record basal conditions for intervals spanning entire glaciations and accessible far from the glacier margins.

After a brief summary of data available from previous reconstructions of the Puget lobe, the basal conditions of the lobe are explored along two complementary lines. We first present calculations of basal drag due to glacier sliding for different models of till bed roughness that indicate that rapid sliding requires very low effective stresses and extensive ice-bed decoupling or ploughing. Second, we summarize geological and geotechnical data that indicate that water pressure beneath the Puget lobe was sufficiently high to allow ploughing of particles and widespread decoupling due to sheetlike water layers at the ice-bed interface.

Reconstructed Velocities and Driving Stress

Balance Velocity

Transverse and longitudinal sections through the Puget lobe at ice maximum, as reconstructed by Thorson [1980], are shown in Figure 3. The ice flux necessary to maintain the warm-based Puget lobe in equilibrium during its maximum extent has been reconstructed by Booth [1986], yielding a balance velocity averaged over a cross section at the equilibrium line, slightly above 1200 m, of 660 m yr^{-1}. Balance velocities varying from 500 to 900 m yr^{-1} were considered plausible based on equilibrium line altitudes (ELAs) ranging from 1100 to 1500 m. Velocity due to internal deformation of the Puget lobe is only 3% of the balance velocity of the glacier [Booth, 1986]. Therefore nearly all of the ice motion resulted from rapid basal
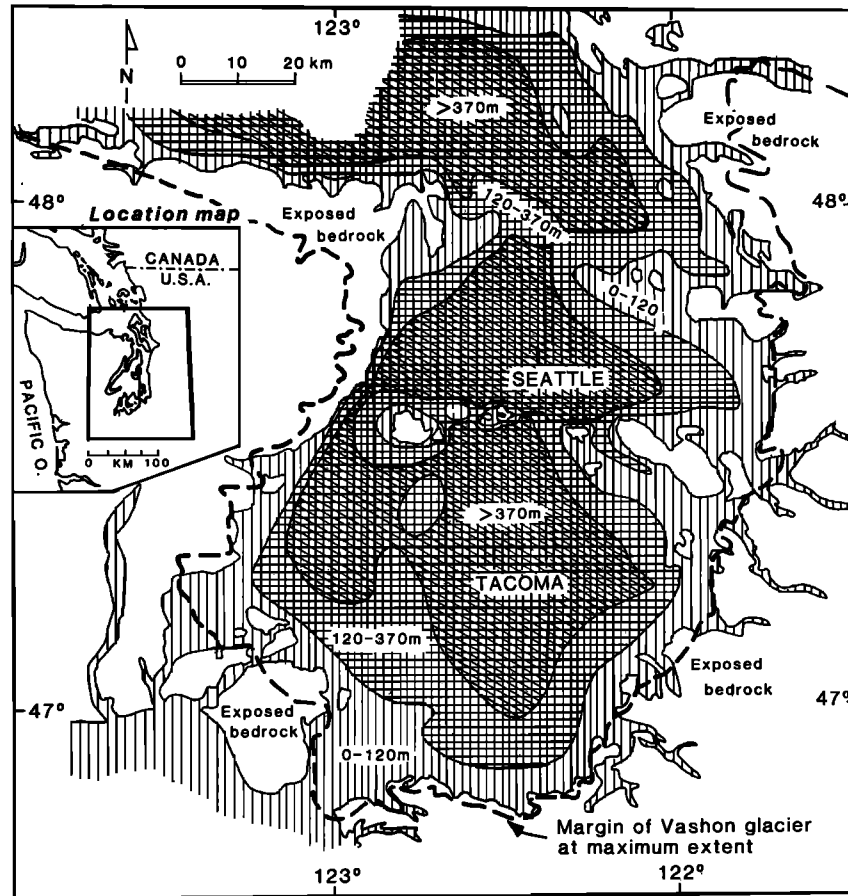
Fig. 1. Map showing nature of the glacier bed. The glacier margin at ice maximum [Thorson, 1980] is indicated by the heavy dashed line. The equilibrium line was located near the top of the figure [Booth, 1986]. Extent of exposed bedrock and thickness of unlithified sediments are from Hall and Othberg [1974]. Approximately 10% of the glaciated area consists of bedrock; roughly 30% of the area is underlain by more than 400 m of sediment.

motion, which may include shearing of the sediments forming the bed, as well as ice sliding over a sediment surface.

The basal velocity of 500 m yr^{-1} is a minimum as long as the ablation and accumulation rates cannot be significantly lower than considered probable by Booth [1986]; errors in glacier area cannot be much greater than those analyzed by Booth [1986]. Significant errors due to climatic changes are not expected because the reconstructed ELAs are consistent with global climate model calculations of regional climate at 12 ka B.P. (J. E. Kutzbach, personal communication, 1986), estimated Vashon age temperatures [Tsukada et al., 1981] and estimates of the temperature and precipitation dependence of the ELA [Porter, 1977]. The use of this minimum sliding velocity in the following calculations will result in a minimum estimated drag.

Driving Stress

Except within 40 km of the terminus, the driving stress τ_d of the Puget lobe, averaged over distances of 20 km:

$$\tau_d = \rho g h \sin\alpha \qquad (1)$$

where ρ is the ice density, g is acceleration due to gravity, h is the ice thickness, and α is the surface slope is about 40 kPa (estimated from surface slope and ice thickness data of Thorson [1980]). Similar low values are characterisic of modern ice sheets [Paterson, 1981, p. 163] and appear to have been common for lobes of the Pleistocene ice sheets [Mathews, 1974].

The driving stress of the Puget Lobe was apparently all supported by basal drag. The width-to-depth ratio is 100, rendering sidewall drag negligible [Paterson, 1981, p. 103]. Minimal longitudinal stress gradients are inferred from the constant driving stress (0.36 ± 0.3 kPa in four sucessive 20-km increments along a flow line) up to 100 km from the terminus. The basal drag calculated for the Puget lobe in the following sections can be compared directly to the inferred driving stress.

Calculated Basal Drag Over a Rigid Bed
of Vashon Till

The basal drag generated by ice sliding, at a specified velocity, over a sediment surface will be affected by conditions that may occur at the bed such as sediment deformation, cavi-
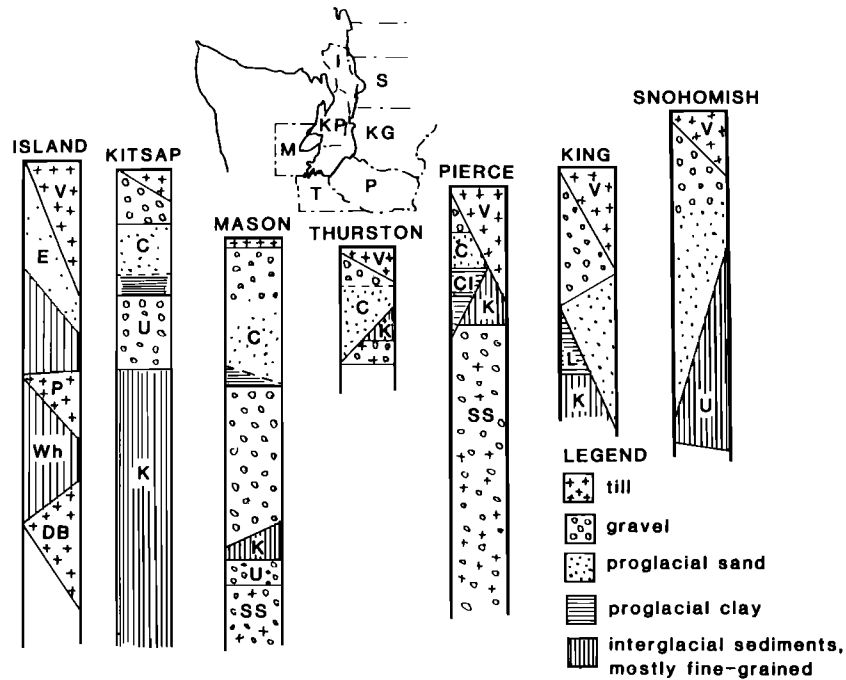
Fig. 2. Puget lowland near-surface stratigraphy is comprised of thick deformable sediments, including from top to bottom (1) Vashon till, (2) gravelly advance outwash and proglacial sand, (3) proglacial clay in the central lowland, (4) thick sequences of preglacial gravel in some areas, and (5) low permeability sediments. Unit thicknesses are presented as maximum and minimum without regard to elevation. The local unit names are indicated by abbreviations: V, Vashon till, E, Esperance sand; C, Colvos sand; L, Lawton clay; K, Kitsap Formation; P, Possession Drift; Wh, Whidbey Formation; DB, Double Bluff Drift; SS, Salmon Springs (?) Drift; U, unnamed [Wallace and Molenaar, 1961; Waldron et al., 1964; Garling et al., 1965; Noble and Wallace, 1966; Easterbrook, 1968; Walters and Kimmel, 1968; Molenaar and Noble, 1970; Minard, 1980].

tation and extensive ice-bed separation. The initial calculation assumes that none of these conditions was present; subsequently, the model is modified to include them.

The basal drag due to ice-molded topography in the Puget lowland is low because ice deformation (creep) is very efficient for such large obstacles, kilometers in length, with low
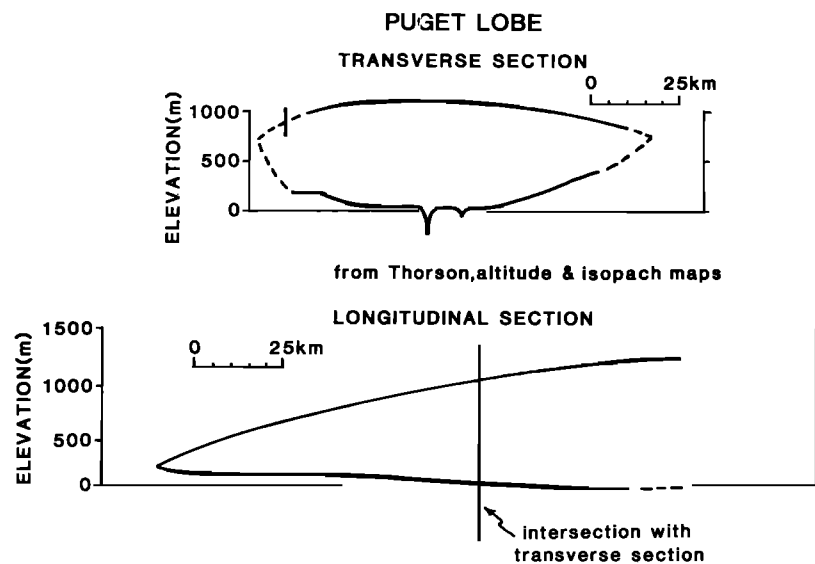

Fig. 3. Transverse and longitudinal section of the reconstructed the Puget glacial lobe at ice maximum. The deepest trough in the transverse section is Puget Sound. The sections intersect in the vicinity of Seattle.
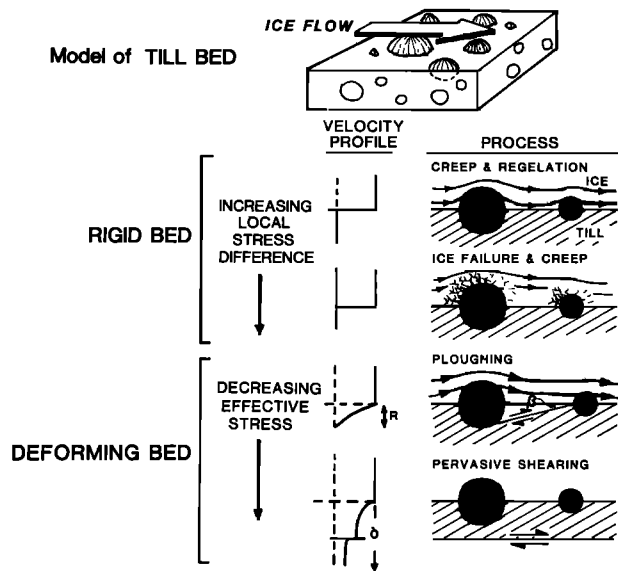
Fig. 4. Schematic portrayal of the hemisphere model of the glacier bed used in the initial basal drag calculation and sections illustrating processes that may have contributed to rapid basal motion of the Vashon lobe. Rigid bed processes of creep and regelation give way to ice failure and creep as local stresses on the obstacles increase with increasing velocity or obstacle size. At low effective stress (high water pressure), deforming bed processes, pervasive shearing, and ploughing prevail.

amplitude-to-wavelength ratios, near 0.1. Contacts between till and underlying sand or outwash gravel are typically very smooth along the ice flow direction. Because these contacts reflect the ice-sediment interface immediately prior to till deposition, the lack of high-amplitude irregularities indicates that the bed was nearly devoid of intermediate-scale roughness, leaving individual grains as the primary contributors of drag. Assuming a rigid bed, sedimentary particles project out of the till surface as roughness elements until they are buried by till aggradation. Stones at the interface project into the ice as knobs; the area between them is a smoother surface composed of sand, silt, and clay. On a smaller scale, sand grains project as knobs and are surrounded by silt and clay. The roughness spectrum will be truncated at the micron scale, corresponding to clay-sized particles that are completely submerged in the basal water film associated with regelation [Hallet, 1979].

Model of the Bed

We begin by assuming that there is no sediment deformation; the bed is rigid and hence ice slides over sediment along a distinct interface. This model is most appropriate at high effective normal stresses. We idealize the particles as spheres centered at the interface (Figure 4). In reality, particles will extend into the ice and the substrate to varying extents; idealizing them as hemispheres provides a convenient average of the resulting

range of particle forms projecting into the ice. Lliboutry's [1978, 1979] model of ice sliding over a rigid, planar surface scattered with hemispherical knobs rigidly fixed on the surface corresponds to this geometric idealization of the glacier bed.

Lliboutry's [1979, equation 46] sliding law is

$$U = B_1 \sigma^n R + C_1 \sigma/R \qquad (2)$$

where U is the sliding velocity, σ is the local shear stress (drag force divided by particle area), R is the obstacle radius, and B_1 and C_1 are constants characteristic of clean glacier ice. The size dependence in this sliding law reflects the fact that creep is most effective for large obstacles; regelation is most effective for small obstacles. For a given sliding velocity, these processes are equally inefficient for some intermediate obstacle size, referred to as the transition size R_*. The transition size decreases with increasing velocity because the effective viscosity of ice decreases with increasing strain rate:

$$R_* = 0.16/U^{1/2} \qquad (3)$$

where R_* and U are expressed in meters and meters per year, respectively [Lliboutry, 1979, equation 45].

The local shear stress reaches a maximum at the transition size and also scales with velocity:

$$\sigma_* = 940\ U^{1/2} \qquad (4)$$

[Lliboutry, 1979, equation 45], where σ_* is in kilopascals. Assuming that particles are rigidly fixed, the local shear stress maximum exceeds the unconfined strength of ice (about 2.5 MPa [Palmer et al., 1983]) for velocites over 7 m yr^{-1}. The failure strength of basal ice, in the presence of water at a pressure approaching the ice overburden pressure, is assumed to equal the unconfined strength of ice. At lower water pressures the ice strength will be higher but is not well-known. The approach taken here is to limit the local shear stress to 2.5 MPa to minimize the estimated basal drag. At high velocities, creep and regelation are not sufficiently effective to accommodate the rapidly moving ice; local stresses sufficient to cause ice failure are generated, and discontinuous ice deformation becomes the dominant process.

Incorporating this ice failure mechanism results in three grain size groups: large particles around which enhanced creep is the dominant process, a transition-size group around R_* for which ice fails locally, and fine particles for which the dominant process is regelation (Figure 5).

Estimated Drag Over Hemisperical Obstacles

The basal drag on the sliding ice mass generated by a planar bed with scattered particles of a single size is ($\sigma \times A_f$), where σ is local shear stress on obstacles of a certain size and A_f is the areal fraction of the bed covered by
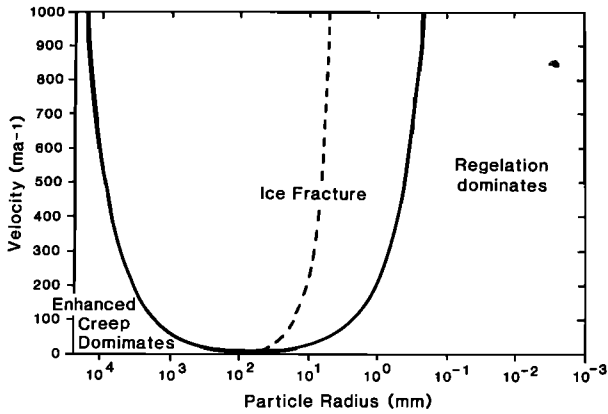
Fig. 5. Obstacle sizes for which local shear stresses reaches 2.5 MPa, taken as the failure strength of the basal ice, as a function of sliding velocity (from Lliboutry's [1979] sliding law). The solid curves divide the size-velocity field into three regions where different sliding processes dominate: regelation for small sizes and low velocities, ice failure for a transition-size group, and creep for large sizes and low velocities. The dashed curve represents the transition size R_*.

those particles. The cumulative basal drag due to particles of different size classes can be approximated as the sum of the individual drag increments:

$$\tau_b = \sum_{i=1}^{m} (\sigma_i \times A_{fi}) \qquad (5)$$

where A_{fi} is the area of the bed composed of particles in size class i, σ_i is the local shear stress for particles of the average size in the class, and m is the number of size classes. Values of σ calculated assuming a velocity of 500 m yr^{-1} are illustrated by the outer solid lines on Figure 6b. Dashed lines represent calculated values of σ that exceed the unconfined failure strength of ice; for particles of these sizes, σ will be set equal to 2.5 MPa.

Equation (5) ignores geometric interference due to superimposition of stress fields where particles are closely spaced. The reduction in drag relative to drag on an isolated sphere (or hemisphere) can be estimated from published numerical results for the drag due to creeping flow of a linear viscous fluid over arrays of closely spaced obstacles. The drag is reduced to 0.1-0.4 of the drag on an isolated hemisphere for configurations including (1) long chains of equal-size particles aligned with the flow whose centers are spaced one to four particle diameters apart [Gluckman et al., 1971], (2) chains of touching particles trending transverse to the flow [Dabros, 1985], and (3) a small sphere in the lee of a larger one with particle volumes differing by 1-2 orders of magnitude [Liao and Kruger, 1980]. The reduction in drag for a linear fluid, when considering particles of all sizes scattered across a plane, is estimated to average 0.25.

The following calculations using this value will tend to underestimate the drag on the glacier because flow deviations around obstacles are expected to be more localized in ice than in linear fluids and are further reduced where regelation facilitates ice motion past obstacles.

The fraction of the bed covered by particles of a given size range, A_f in equation (5), can be determined from the grain-size distribution of the sediment. The grain size distribution used, an average of data for eight samples from the Vashon till in the Seattle area, is plotted as weight fraction in a given size class in Figure 6a. Size classes of log (R_1/R_2) = 0.1, where R_1 and R_2 are the class limits, were used. The logarithmic mean of each size class was taken as the particle size for which σ_i was calculated.

Volumetric fraction was found to be not significantly different from areal fraction for this poorly-sorted sediment. The areal frac-
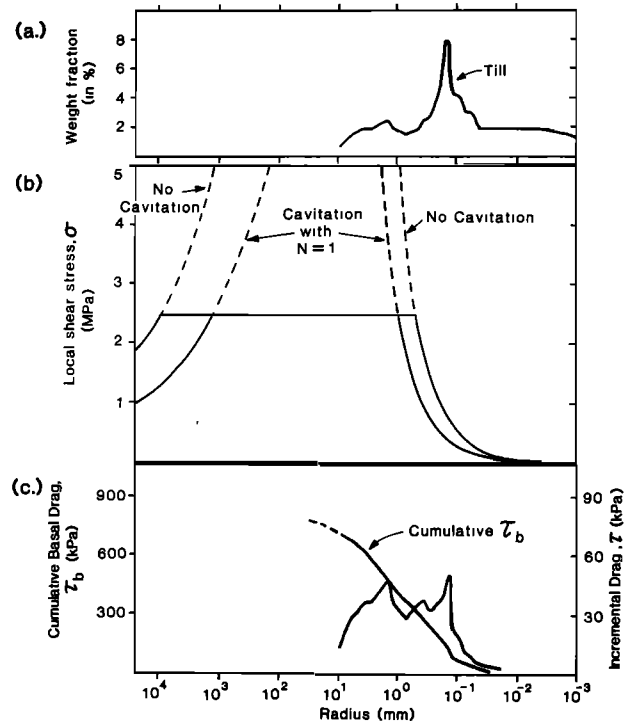

Fig. 6. Calculation of basal drag generated by a rigid bed of till without cavitation. The fraction of sediment in size classes such that log(R_2/R_1)=0.1, where R_1 and R_2 are the size class limits, of a representative till grain size distribution (shown in Figure 6a) is multiplied by the local shear stress (shown in Figure 6b) to obtain the total basal drag (shown in Figure 6c). Total basal drag is plotted both as increments obtained for each grain-size class and as a cumulative curve. The coarse mode of the bimodal grain-size distribution is relatively weak but contributes as much drag as the fine mode due to the high local shear stress on particles of this size. Geometric interference effects would reduce the cumulative drag to about 600 kPa.

tion covered by an individual size class can then be obtained by converting weight fraction W_f to volumetric fraction V_f:

$$V_f = W_f \times (1-n) \qquad (6)$$

where n is the sediment porosity. Based on a void ratio (void volume/solid volume) of 0.3 for Puget Lowland tills (range 0.25-0.35; [Easterbrook, 1964]), (1-n) averages 0.77.

The basal shear stress obtained by the above method, without correcting for closely spaced particles, is about 800 kPa (Figure 6c) with the following assumptions: a rigid bed, velocity of 500 m yr^{-1}, a 1-μm water film, and local shear stress not exceeding the unconfined failure strength of ice. As the local shear stress with regelation and creep at a velocity of 500 m yr^{-1} would generally exceed the failure strength of ice, the local shear stress in the calculation is limited to the ice strength for a large fraction of the particles. This occurs for sizes near the transition size; no particles in the Vashon till sample are in the group for which creep predominates so the transition-size group includes all particles greater than 0.4 mm in radius or 28% of the sediment.

Because the interference effect due to closely spaced particles applies to the local shear stress in the absence of ice failure, the interference factor, 0.25, must be applied before the local shear stresses are limited to the failure strength of the ice. The drag increments due to a large fraction of the sediment will be unchanged because the reduced local shear stress still exceeds the failure strength of the ice. For somewhat smaller particles the reduced local shear stress drops below the failure strength of ice but is still greater than a quarter of the previously calculated drag increment where the local shear stress was set equal to the failure strength of ice. Only for the finest particles can the previously calculated drag increments be directly multiplied by 0.25. Because only a small fraction of the drag increments are reduced to a quarter of their previous value, the drag for the Vashon till is reduced only to about 600 kPa when geometric interference is accounted for. This estimate of the drag is an order of magnitude greater than the inferred driving stress, in spite of being intentionally minimized by the choice of assumed velocity, ice strength, and a geometric interference factor appropriate for linear fluids.

Basal Drag With a Smoothed Rigid Bed

As the obstacles at the bed have been modeled as hemispheres, it is of interest to assess the drag on smoother beds where large grains protrude only slightly into the ice. Nye's [1969] model for sliding over low roughness beds provides a convenient means of estimating the drag over two such beds whose simple roughness spectra capture the essence of a mechanically smoothed till surface. First, a constant amplitude roughness spectrum depicts grains of all sizes as protruding a fixed height z_0 into the ice. This spectrum is truncated above wavelengths corresponding to the largest particles and below wavelengths corresponding to the smallest particles that can reasonably provide roughness of the given amplitude. The second smoothed bed model again assumes that large grains are centered well below the interface but allows the effective amplitude to increase with the wavelength. We assume that the amplitude scales with the wavelength, and hence this model corresponds to a white roughness bed [Nye, 1970]. For the uniform amplitude bed, assuming (1) a sliding velocity of 500 m yr^{-1}, (2) a reasonable characteristic height z_0 of 1 mm, (3) a maximum size of 0.1 m, (4) a transition size of 10 mm, and (5) an effective viscosity of 100 kPa yr, the resulting basal drag is 0.9 MPa. For the white roughness bed the drag is 3 MPa with similar assumptions. Thus even with greatly smoothed beds, the drag is much higher than the reconstructed driving stress and processes that decouple the ice from the bed must be considered.

Estimated Drag With Cavitation

The drag in the case of cavities localized at the lee of individual particles is estimated following Lliboutry [1979], assuming that the normal stress on the stoss of obstacles is the same as for no cavitation and the stress on the lee falls to the water pressure. Cavitation will occur where the total normal stress on the lee of an obstacle is less than the water pressure, that is where the effective stress on the lee of the obstacle N_{ls} vanishes. As the normal stress fluctuation averaged over the lee of a hemisphere roughly equals the local shear stress σ [Lliboutry, 1978], this will occur where σ exceeds the far-field basal effective stress N. The size range of particles behind which cavities form can be found by substituting N into the sliding law (equation (2):

$$U = B_1 R N^n + C_1 (N/R) \qquad (7)$$

The roots of this equation give the upper and lower limits of cavitation provided N is less than both σ and the failure strength of ice. From equation (6), assuming a glacier sliding at 500 m yr^{-1}, cavitation will occur over immobile particles of essentially all sizes if the effective stress is 100 kPa or less.

Values of σ with N = 100 kPa are shown by the inner solid lines in Figure 6b. In this case, the drag over the Vashon till bed is about 400 kPa, or 300 kPa when adjusted for geometric interference. These values are still an order of magnitude larger than the reconstructed driving stress; hence localized cavities do not appear to account for the rapid motion of the glacier.

Comparison With Experiments

Experiments by Budd et al. [1979] with ice sliding over a rigid slab manufactured of pebbles 5-10 mm in radius suggest basal shear stresses between 150 and 200 kPa at low effective stresses (350-450 kPa) when the sliding velocities are extrapolated to 500 m yr^{-1}. The

drag was also found to be inversely proportional to the effective stress; adjusting to an effective stress of 100 kPa, the above experimental data indicate a basal drag of about 45 kPa. Thus the experimental results vary by an order of magnitude from the drag calculated here, presumably because large local stresses give rise to much lower effective ice viscosities and extensive cavities may decouple a large fraction of the particles from the ice. For a velocity of 500 m yr^{-1} the basal drag would be reduced by an order of magnitude if about 90% of the bed was decoupled from the ice. Thus the experiments indicate that large ice sheets could slide very rapidly over a rigid bed at low effective stresses. However, for the Puget lobe the deformable sediment would not have remained rigid at such low effective stresses.

Estimated Drag with a Deforming Bed

As the water pressure approaches the ice overburden pressure and effective stress decreases, ploughing of sedimentary particles coupled to the ice at the interface, ice-bed separation, and, finally, pervasive shearing become possible, as sketched in Figure 4. Drag with ploughing and ice-bed separation will be calculated by modifying the above model. Pervasive shearing will be considered in terms of the relevant geologic evidence.

Model of Ploughing

Stress will be concentrated on particles projecting into the ice above the till surface. Such particles will tend to move and hence to plough through the substrate. The conditions necessary for the occurrence of ploughing can be analyzed by considering a particle, partly buried in fine sediment. The particle will plough through the surrounding sediment if the force exerted by ice flow exceeds the force resisting local sediment failure. For an idealized spherical particle half-buried in sediment, the failure surface can be approximated as half of a cone extending from the base of the particle to the sediment surface (Figure 4). Due to the large shear traction exerted on particles parallel to the sediment surface, the principal compressive stress direction is expected to be essentially aligned with the flow direction. The angle between the failure surface and the sediment surface β is expected to approximate the angle between the maximum principal stress and the failure surface, $(45 - \phi/2)$, where ϕ is the internal friction angle of the sediment. The average shear stress τ_f on this hemiconical surface is approximately the drag force ($F_d = \sigma\pi R^2$) divided by the failure surface area:

$$\tau_f = 2\sigma \tan(45 - \phi/2) \qquad (8)$$

The strength of the failure surface varies with the effective stress in the lee of the obstacle N_{1f}. Using the Mohr-Coulomb failure criterion, the strength of the sediment s is

$$s = c + N_{1f} \tan\phi \qquad (9)$$

where c is the cohesion. The cohesion is expected to contribute little strength except at negligible effective stresses and will be set to zero in the following analysis.

A ploughing index P_*, such that ploughing will occur when the index is greater than unity, can be defined as the ratio of the local applied stress to the sediment strength, which reduces to

$$P_* = a_1(\sigma/N_{1f}) = a_2(\sigma/N) \qquad (10)$$

where a_1 is $[2 \tan(45-\phi/2)/\tan\phi]$. Local normal stresses over the failure plane will differ from the farfield normal stress, N by an amount $(k\sigma)$, where k is an interger. Therefore a_2 equals (a_1+k). Based on the average of the circumferential stress generated by ice deformation over the midline of the failure surface [Lliboutry and Ritz, 1978], the proportionality factor k will be 0.44 and 0.39 where ϕ is 20° and 30°, respectively. Based on the average of the circumferential stresses produced by regelation [Nye, 1968], the proportionality will be 0.12 and 0.10 where ϕ is 20° and 30°, respectively. The value of a_2 varies with ϕ for the two cases as

	$\phi=20°$	$\phi=30°$
a_2, for creep	4.3	2.4
a_2, for regelation	4.0	2.0

The ploughing criterion indicates that ploughing is suppressed and particles of all sizes can lodge, when effective stresses are high. Because σ must not exceed the failure strength of ice and a_2 is generally greater than 1, the maximum effective stress consistent with ploughing exceeds the failure strength of ice, for example, by a factor of 2.0 to 2.4 when $\phi = 30°$. At effective stresses N below this level, particles of intermediate size, for which the sliding law predicts a local shear stress, $\sigma > (1/a_2)N$, will plough through the sediment. Ice must move past these ploughing particles at a rate just sufficient to generate the viscous drag required to maintain ploughing. This places an upper limit, $\sigma = (1/a_2)N$, on the local shear stress and supresses cavitation at the lee of moving clasts because the $\sigma > N$ criterion for cavitation is generally not satisfied.

The ploughing criterion has very important implications for the grain-size distribution of tills. Where the substrate is solid rock, particles surrounded by ice can lodge only at very low sliding velocities. Except for very large boulders, the process is independent of particle size because the forces inducing and resisting motion scale, in the same manner, with particle size [Hallet, 1981]. In contrast, where particles in the ice can become partially embedded in a deformable substrate, whether due simply to till aggradation or by being pressed into the bed during times of low effective stress, a fraction of those particles will remain lodged. Whether particles are remobilized or lodged will depend on grain size. For rapid sliding over a till containing particles both larger and smaller than the
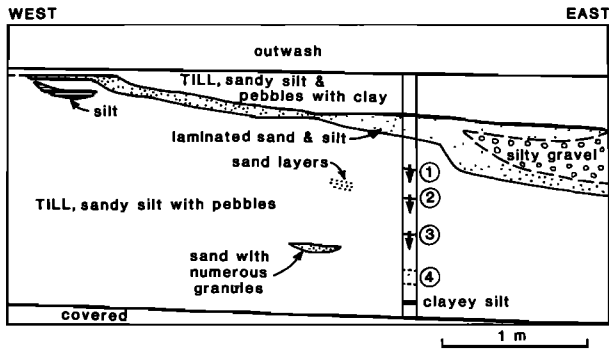
Fig. 7. Section showing intratill channel fill composed of interlaminated fine to medium sand to clayey silt. The four numbered points on the indicated column of till mark till layering, apparently reflecting varying water pressure and extent of ice-bed separation, in which texture varies downward as follows: (1) increasing granules and small pebbles, (2) decreasing granules and pebbles, (3) increasing sand, and (4) layer of sand or very sandy till.

transition size group, increasing effective stress and decreasing velocity will be recorded by an increase in the proportion of particles in two size fractions: one coarser and one finer than the transition size. For example, a_2N increasing from 1 to 2 MPa will lead to increased deposition of small boulders and coarse sand. The wide range of till grain size distributions in a given area [Sugden and John, 1976], including the Vashon till [Olmsted, 1969] and the layered nature of the Vashon till (Figure 7) and other tills, may be due in part to this process.

Estimated Drag With Ploughing

With ploughing, the drag generated by coarse particles at the bed of the Puget lobe will be reduced to a value determined by the failure strength of the sediment. A basal drag near 40 kPa can be obtained when the sediment strength limits the maximum local shear stress on ploughing particles to 100 kPa. In this case, all particles larger than about 0.1 mm must plough; they cover 44% of the bed and contribute a drag of 44 kPa. Drag from smaller particles is negligible. A local shear stress maximum of 100 kPa implies effective normal stresses around 200 kPa (roughly twice the local shear stress on the ploughing particles based on the ploughing index and assuming $\phi = 30°$) or water pressure greater than or equal to 98% of the ice overburden at the maximum extent of the Puget lobe.

Drag With Water Layers

The process of ploughing is sufficient to allow the rapid motion of the Puget lobe with low basal drag; however, such low basal effective stresses also favor extensive ice-bed separation. A basal water layer of uniform thickness would eliminate the drag due to the smallest particles by decoupling them from the ice. In addition, such water layers would reduce the fraction of the sediment which must plough and consequently increase the effective stress consistent with glacier motion of 500 m yr^{-1}. Uniform water layers of greater than a few millimeters in thickness are likely to be unstable [Walder, 1982] and are not considered. Local shear stresses of 500 kPa, on the 7.5% of the bed coarser than 3 mm radius, are consistent with a basal drag of 40 kPa. Based on the ploughing index, local shear stresses will be maintained at this low level by ploughing when the effective stress is 1.0 MPa, corresponding to 90% of the 10 MPa ice overburden.

Geologic Evidence of Basal Conditions

Characteristics of the subglacial sediments can constrain the models used in the previous section by allowing us to (1) estimate subglacial water pressure, (2) reconstruct elements of the subglacial hydrology, and (3) evaluate the importance of pervasive shearing as a contribution to glacier motion.

Long-Term Average Water Pressure

Overconsolidation of proglacial clays that underlay the Puget lobe can be used to determine the minimum water pressure, corresponding to the maximum effective stress to which they have previously been subjected. The response of saturated clays to water pressure variations is a diffusion-type process [Terzaghi and Peck, 1967] in which water pressure fluctuations at the sediment surface are transmitted to the underlying material. The response is analogous to the diffusive thermal response in an infinite half-space with periodic heating at the surface [Carslaw and Jaeger, 1959]. The amplitude of the variation decreases exponentially with depth and the damping scales with the frequency. The skin depth w at which the amplitude is reduced to $1/e$ of the surface amplitude is

$$\delta - (c_v T/\pi)^{1/2} \qquad (11)$$

where c_v is the hydraulic diffusivity and T is the period of the variation [Turcotte and Schubert, 1982].

The diffusivity, also called the coefficient of consolidation, is

$$c_v = [k\ N_{av}]/0.435\ c_c\ \rho_w\ g \qquad (12)$$

where k is hydraulic conductivity, N_{av} is the average effective stress, c_c is a compression index, and ρ_w is the water density [Lambe, 1951]. Hydraulic conductivity is approximately 10^{-8} m s^{-1} for the Vashon till [Olmstead, 1969]; it is expected to be of the order of 10^{-9} m s^{-1} [Freeze and Cherry, 1979] for the Lawton clay, the proglacial clay underlying the Seattle area. For the Lawton clay, $c_c = 0.27(1 + e_o)$, where e_o is the initial void ratio (G. Denby, 1986, personal communication,) and is

not expected to vary widely [Lambe, 1951, Table IX-1];. Using these values, the diffusivity appropriate for considering water pressure variations at the ice-till interface beneath the Puget lobe, assuming a pressure variation amplitude equal to the maximum ice overburden in the Seattle area, 0-10 MPa, is 4.4×10^{-4} m^2 s^{-1} for the till and 7.8×10^{-6} m^2 s^{-1} within the Lawton clay. These hydraulic diffusivities give skin depths of 28 and 9 m in the till and clay, respectively, for annual pressure variations on a annual cycle and 8 and 6 m, respectively, for monthly fluctuations. Assuming that the range of water pressures likely for the Puget lobe will be from zero to some maximum value, smaller skin depths would be obtained for lower-amplitude pressure fluctuations.

Preconsolidation pressures for the Lawton clay in the Seattle area [LaPrade, 1982] average 1 MPa and reach a maximum of 3 MPa. The calculated skin depths indicate that all samples tested, from 2 to 42 m from the nearest drainage layer, would reflect fluctuations in effective stress that last years or longer. It follows that the water pressure beneath the Puget lobe did not drop below 90% of the ice overburden for time periods in excess of 1 year and ploughing would have been a characteristic process.

Subglacial Drainage Through Aquifers

Theoretical constraints on the subglacial movement of water indicate higher subglacial water pressures, approximating the ice overburden, would have been common. Water reaching the glacier bed will be derived from surface melting, basal melting due to frictional heating and due to geothermal melting [Lliboutry, 1979]. For the Puget lobe, by far the largest quantity of water reaching the bed will be due to surface melting. The mass balance curve appropriate for this glacier indicates about 2.5 m yr^{-1} ablation in the vicinity of Seattle at ice maximum [Booth, 1986]. A portion of this water may have drained across the glacier surface; however, a large quantity would have reached the bed through moulins. Water generated by frictional heating can be estimated from the energy loss of the glacier as $(\tau_b \times U)/L$, where L is the volumetric latent heat due to ice melting. At an ice velocity of 500 m yr^{-1}, 66 mm yr^{-1} of water would be produced. Very little water is produced by geothermal melting, about 3 mm yr^{-1} using the present-day geothermal heat flux in the Puget Lowland (26 mJ m^{-2} yr^{-1} [Washington Department of Natural Resources, 1981]).

Ignoring for the moment large water input from the glacier surface, high pore water pressure will be generated away from the ice margin to maintain sufficiently high hydraulic gradients to drain even a portion of the basal meltwater to the marginal zone. Although up to 400 m of unconsolidated sediments underlie much of the Lowland (Figure 1), deep wells [Liesch et al., 1963; Noble and Wallace, 1966; Easterbrook, 1968] record a stratigraphy of several-100-m-thick clay layers alternating

with zones of thinner, interlayered sand and clay. As a rough estimate, 100 m of permeable sediments underlay the glacier. Assuming (1) a 100 m thick permeable layer acting as an aquifer beneath the till and (2) meltwater entering this aquifer along the full length of the glacier, the pore pressure gradient required to drain the water can be determined from continuity and Darcy's law [Booth, 1984]. Hydraulic conductivity of the near-surface proglacial sand ranges from about 10^{-2} to 10^{-5} m^2 s^{-1} based on data from one area [Griffin et al., 1962], as expected for most sands [Freeze and Cherry, 1979]. Using the average of these hydraulic conductivities, the hydraulic head would reach the height of the glacier surface in the vicinity of Seattle, about 150 km north of the terminus, with an aquifer 100 m thick draining about half the water produced by basal melting alone.

Because subglacial aquifers were not sufficiently thick to drain the basal meltwater, pore water pressure in the subglacial sediments can be expected to approach the ice overburden beneath much of the glacier. Similar models have shown basal water pressure tending to be very high away from glacier margins [Boulton et al., 1974; Shoemaker, 1986; Lingle and Brown, 1987], but all have dealt with much thinner or less permeable aquifers and more limited water input.

Evidence of Subglacial Tunnels

Subglacial water not draining through aquifers must have drained at the interface: in a limited number of tunnels or distributed across the beds in interconnected water layers covering a significant portion of the bed. The existence of tunnels will not invalidate the aquifer drainage calculation because the water pressure in tunnels will be close to that over the remainder of the bed. In steady state tunnels beneath temperate ice, the water pressure is generally somewhat lower than the ice pressure because melting of tunnel walls due to viscous dissipation must be compensated by radial convergence of ice toward the tunnel; however, in water-filled conduits under thick ice, the difference in pressure will be slight [Shreve, 1972]. Due to the permeability of the interface, the pore water pressure and the pressure in water layers distributed across the bed are also likely to closely approach the ice pressure.

Channel deposits observed within the Vashon till indicate subglacial tunnels ranged from less than 0.1 m to 8 m in horizontal extent (Figure 7). The estimated annually averaged water flux beneath the Puget lobe varies from 1000 to 3000 m^3 s^{-1} between the glacier terminus and the vicinity of Seattle at ice maximum [Booth, 1986]. As a rough estimate, 20-60 tunnels would be sufficient to drain the surface meltwater if they were of the maximum size observed in the Vashon till and of the form assumed by Shreve [1972]; these numbers correspond to a spacing of 2-5 km. Such tunnels would be located between the subglacially stream-lined ridges that are spaced several
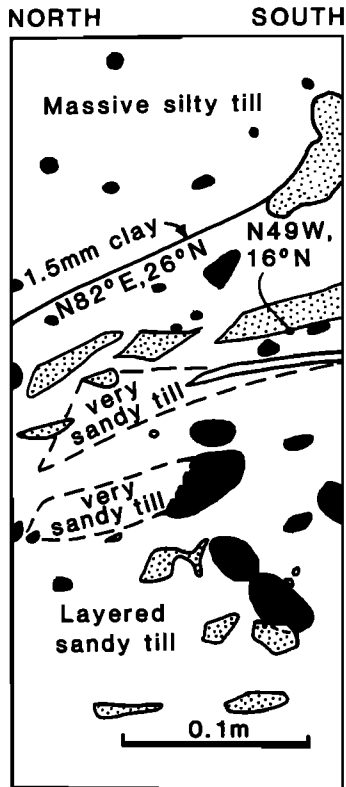
Fig. 8. Section showing a portion of a massive silty till zone separated from the underlying layered sandy till by a thin clay layer, possibly a shear zone. Tabular sorted sand bodies within the till (the stippled pattern) appear to be segments of two sand layers indicating sediment deformation and, therefore high water pressure, but reflecting limited shear strain. Solid areas are pebbles in the till.

kilometers apart in the Seattle area, in accord with the spacing inferred based on water flux and tunnel size. Similar tunnel spacings were inferred from bedrock topography near the eastern margin of the lobe [Booth, 1987].

Subglacial Shearing as a Contribution to Glacier Velocity

It has frequently been recognized in the glaciological literature that high water pressure is required for shearing of subglacial sediment [Boulton et al., 1974; Menzies, 1979; Smalley, 1981]. Equation (8) provides the appropriate relationship between the normal effective stress and the shear stress at which the material will fail. Values for ϕ and c have been obtained for five New England tills; tan ϕ ranged from 0.6 to 0.8, while c varied from 0 to 40 kPa (consolidated undrained tests [Linell and Shea, 1960]). These data indicate the range of ϕ values likely for till and that cohesion is likely to be low. The plausible minimum for tan ϕ is about 0.2 [Terzaghi and Peck, 1967, pp. 112]. Because the shear stress exerted on the sediment beneath large glaciers and ice sheets averages about 50 kPa [Paterson,

1981, p. 63], the Mohr-Coulomb failure criterion indicates that subglacial sediments will not shear unless pore water pressure is very high, resulting in an effective normal stress less than 100 kPa. For the Vashon till in the vicinity of Seattle, this low effective stress corresponds to a water pressure equal to 99% of the ice overburden at ice maximum. That this water pressure was achieved beneath the Puget lobe is indicated by the deformation features recorded within it (Figure 8).

At the very low basal effective stresses inferred for the Puget lobe, the possibility of pervasive shearing of the subglacial sediment must be considered. Assuming that all the basal motion was due to substrate shearing, cumulative shear strain recorded in the till would be extremely high, roughly 10^5. This figure is based on assuming an average sliding rate of 500 m yr^{-1}, continuing for 1500 years, and deformation distributed through the entire till thickness of 15 m.

Numerous sorted sediment bodies contained in the Vashon till are likely to have been present from the moment the till horizon was deposited and, therefore, subjected to a strain history similar to that of the rest of the till. Although some of these sorted sediments could have been sheared up into the till from the underlying sediments, subglacial deposition is indicated by the concentration of these sediments near the middle of the till. These sediments occur as extensive subhorizontal layers in zones up to 25 m in horizontal extent, 1 mm to 0.3 m thick tabular bodies in various orientations, and 10 mm to 1 m relatively equidimensional pods. The range of forms is consistent with their originating from subhorizontal layers that have been segmented and subjected to various strains; at several locations where deformation appears limited the apparent original form of subhorizontal or folded layers can be inferred. The minimal shear strain indicated by the offset of layer segments in Figure 8, on the order of 1 or less, is typical. The abundance of sorted sediment structures within the till that have not been attenuated into thin streaks by extensive shear strain implies shear strain magnitudes are generally orders of magnitude less than 10^5. This evidence against large shear strains implies that pervasive shearing of the till did not contribute significantly to the basal motion of the glacier. However, shearing along discrete shear zones is evident and may amount to significant displacement (Figure 8).

Ice-Bed Separation

The low effective stress reconstructed for the Puget lobe implies widespread ice-bed separation and the formation of water layers at the bed. Basal water in such layers will be recorded in the till as long as water flow sorts sediment sufficiently to differentiate it from the surrounding till. The Vashon Till contains layers and lenses of sorted sediment in 80% of the 25 outcrops examined in the Seattle area. Similar sorted sediments have been described in Vashon till throughout the Puget lowland [Noble and Wallace, 1966;

Easterbrook, 1968; Minard, 1980; Booth, 1984] and in other areas [Shaw, 1979; Eyles et al., 1982]. In the Vashon till, these sedimentary features reflect water covering a significant portion of the bed and a wide range of water flow velocities.

Layered till occurs in a quarter of the 25 sites investigated. Adjacent layers are distinguished by slight textural differences: typically observed as varying moisture or pebble content. The layers are discontinuous but vary in horizontal extent from a few meters to greater than 30 m and up to 1.3 m thickness. Pebbly layers were repeated at intervals of 0.2-0.3 m in one section, implying a cyclic occurences of the conditions for deposition of numerous pebbles.

The till layering appears to result from slight sorting by slowly flowing water at the interface, in combination with selective lodgement of pebbles. Pebble-poor till layers would be formed at relatively high water pressure when most pebbles would plough through the underlying sediment. At such high water pressure, flow in thin water layers would begin to sort the sediment by removing fines.

The sorted sediment structures found in roughly 60% of the outcrops are considerably better sorted than the enclosing till and range from predominantly clay to gravel and from well to poorly sorted. Because of the lack of a channel form and the coarse grains sizes included, these sediments appear to record deposition from water flowing in broad sheet-like layers under the ice.

Considering only the sorted sediments, the ice-bed separation and low effective stresses they imply were a widespread condition at the bed of the Puget lobe. The volumetric fraction of the sorted sediments estimated from till exposures, assuming that long-term average rate of deposition of both till and sorted sediments is equivalent, represents a temporal average of the proportion of the bed covered by water. Sorted sediments typically comprise only 1-10% of the till exposure. Near the central portion of the till (presumably when the glacier was near its maximum extent), the proportion of sorted sediment reaches 15 to as much as 30% of the outcrop. Hence a large fraction of the bed appears to have been covered with water layers sufficiently thick to allow transport of sand and occasionally gravel. Areas covered by such water layers provide little resistance to ice motion.

Conclusions

The basal drag generated by a glacier sliding at 500 m yr^{-1} over the Vashon till has been calculated as 600 kPa assuming a rigid bed, no cavitation, and taking into account close spacing of particles in the till. The average driving stress of the late Pleistocene Puget lobe is inferred to be about 40 kPa, an order of magnitude less than the calculated drag. Ploughing at the interface could reduce the drag to the reconstucted value if a large fraction of the particles plough. The high water pressures required for ploughing will, at the same time, allow the presence of submillimeter-

thick water layers that further reduce the drag by submerging the smaller particles.

Data from sediments that underlay the former Puget lobe indicate that long-term minimum water pressures exceeded 90% of the 10 MPa ice overburden. The inability of subglacial aquifers to drain all the water reaching the bed indicate even higher subglacial water pressures. Water reaching the bed by basal melting probably coalesced into a system of interconnected water layers before reaching a tunnel system with a characteristic spacing of kilometers. Alternating pebble-rich and pebble-poor layers of till, with associated differences in matrix texture, may reflect cyclic water pressure variations and formation of thin water layers, as well as differential lodgement. During the glacier maximum, water pressures probably reached the ice overburden causing widespread ice-bed separation and formation of extensive water layers, up to centimeters in thickness, over roughly 10-15% of the bed. Deformation structures in the till indicate basal water pressures near 99% of the maximum ice overburden but insufficient shear strain for pervasive till deformation to have contributed significantly to the glacier motion.

Reconstruction of former ice sheets and inferences based on characteristics of glaciogenic sediments provide valuable insights into the dynamics of glaciers on deformable beds. Sediment characteristics permit assessment of former basal shear stresses, substrate shear strains, and effective stresses that have the same order of accuracy as those from studies of modern glaciers. Moreover, the magnitudes of shear and effective stresses inferred by both types of studies are similar.

References

Anderson, H. W., Groundwater resources of Island Co., vol. II, Water Supply Bull. Wash. Dep. Water Resour., 25, 317 pp., 1968.
Armstrong, J. E., D. R. Crandell, D.J. Easterbrook, and J. B. Noble, Late Pleistocene stratigraphy and chronology in southwestern British Columbia and northwestern Washington, Geol. Soc. Am. Bull., 76, 321-330, 1965.
Blankenship, D. D., C. R. Bentley, S. T. Rooney, and R. B. Alley, Seismic measurements reveal a saturated, porous layer beneath an active Antarctic ice stream, Nature, 322, 54-57, 1986.
Booth, D. B., Glacier dynamics and the development of glaciated landforms in the Eastern Puget Lowland, WA, Ph.D. dissertation, 217 pp., Univ. of Wash., Seattle, 1984.
Booth, D. B., Mass balance and sliding velocity of the Puget lobe of the Cordilleran ice sheet during the last glaciation, Quat. Res., 25(3), 269-280, 1986.
Booth, D. B., Surficial geology of the Skykomish and Snoqualamie Rivers area, Snohomish and King Counties, Washington, U.S. Geol. Surv. Geol. Invest. Map, I-1745, in press, 1987.
Boulton, G. S., D. L. Dent, and E. M. Morris, Subglacial shearing and crushing and the role of water pressures in tills from southeast Iceland, Geogr. Ann., Ser. A, 135-145, 1974.

Budd, W. F., P. L. Keage, and N. A. Blundy, Empirical studies of ice sliding, J. Glaciol., 23 (89), 157-170, 1979.

Carslaw, H. S., and J. C. Jaeger, Conduction of Heat in Solids, 2nd ed., Clarendon Press, London, 1959.

Dabros, T., A singularity method for calculating hydrodynamic forces and particle velocities in low-Reynolds-number flows, J. Fluid Mech., 156, 1-21, 1985.

Easterbrook, D. J., Void ratio and bulk densities as a means of identifying Pleistocene tills, Geol. Soc. Am. Bull., 75, 745-750, 1964.

Easterbrook, D. J., Pleistocene stratigraphy of Island Co., vol. I, Water Supply Bull. Wash. Dep. Water Resour., 25, 34 pp., 1968.

Eyles, N., J. Sladen, and S. Gilroy, A depositional model for stratigraphic complexes and facies superimposition in lodgement tills, Boreas, 11, 317-333, 1982.

Freeze, R. A. and J. A. Cherry, Groundwater, 604 pp., Prentice- Hall, Englewood Cliffs, N.J., 1979.

Garling, M. E., D. Molenaar, A. S. Denburgh, and G. H. Fiedler, Water resources and geology of the Kitsap Peninsula and certain adjacent islands, Water Supply Bull. Wash. Dep. Water Resour., 18, 309 pp., 1965.

Gluckman, M. J., R. Pfeffer, and S. Weinbaum, A new technique for treating multiparticle slow viscous flow: Axisymmetric flow past spheres and spheroids, J. Fluid Mech., 90(4), 705-740, 1971.

Griffin, W. C., J. E. Sceva, H. A. Swenson, and M. J. Mundorff, Water resources of the Tacoma area, Water Supply Bull. Wash. Dep. Water Resources, 19, 101 pp., 1962.

Hall, J. B., and K. L. Othberg, Thickness of unconsolidated sediment, Puget Lowland, WA, Geol. Map GM-12, Dep. of Nat. Resour., Div. of Geol. and Earth Resour., State of Wash., Olympia, 1974.

Hallet, B., Subglacial regelation water film, J. Glaciol., 23(89), 321-334, 1979.

Hallet, B., Glacial abrasion and sliding: Their dependence on the debris concentration in basal ice, Ann. Glaciol., 2, 23-28, 1981.

Kamb, B., C. F. Raymond, W. D. Harrison, H. Engelhardt, K. A. Echelmeyer, N. Humphrey, M. M. Brugman, and T. Pfeffer, Glacier surge mechanism: 1982-1983 surge of the Variegated Glacier, Alaska, Science, 227(4686), 469-479, 1985.

Lambe, T. W. Soil Testing for Engineers, 165 pp., John Wiley, New York, 1951.

LaPrade, W. T., Geologic implications of pre-consolidated pressure values, Lawton Clay, Seattle, Washington, in Proceedings of 19th Annual Engineering, Geology, and Soils Engineering Symposium, 303-321, Idaho State University, Pocatello, 1982.

Liao, W. and D. A. Krueger, Multipole expansion calculation of slow viscous flow about spheroids of different sizes, J. Fluid Mech, 96(2), 223-241, 1980.

Liesch, B. A., C. E. Price, and K. L. Walters, Geology and groundwater resources of Northwestern Ring Co., Washington, Water Supply Bull. Wash. Dep. Water Resour., 20, 240 pp, 1963.

Linell, K. A., and H. F. Shea, Strength and deformation characteristics of various glacial tills in New England, in ASCE Research Conference on the Shear Strength of Cohesive Soils, pp.275-314, American Society of Civil Engineers, Boulder, Colo., 1960.

Lingle, C. S., and T. J. Brown, A subglacial aquifer bed model and water pressure-dependent basal sliding relationship for a West Antarctic ice stream, in Dynamics of the West Antarctic Ice Sheet, edited by C. J.Van der Veen and J. Oerlmans, D. Reidel, Norwell, Mass., in press, 1987.

Lliboutry, L., Glissement d'un glacier sur un plan parseme d'obstacles hemispheriques, Ann. Geophys., 34(2), 147-162, 1978.

Lliboutry, L., Local friction laws for glaciers: A critical review and new openings, J. Glaciol., 23(89), 67-95, 1979.

Lliboutry, L., and C. Ritz, Ecoulement permanente d'un fluide visqueax nonlineaire (corps de Glen) autour d'un sphere parfaitment lisse, Ann. Geophys., 34(21) 133-146, 1978.

Mathews, W. H., Surface profiles of the Laurentide ice sheet in its marginal areas, J. Glaciol., 13(67), 37-43, 1974.

Meier, M. F., W. V. Tangborn, L. R. Mayo, and A. Post, Combined ice and water balances of Gulkana and Wolverine glaciers, Alaska and South Cascade glacier, Washington, 1965 & 1966 hydrologicl years, U.S. Geol. Surv. Prof. Pap., 715A, 23 pp., 1971.

Menzies, J. G., The mechanics of drumlin formation with particular reference to the change in pore-water content of the till, J. Glaciol., 22(87), 373-383, 1979.

Minard, J. P., Geology of the Maltby Quadrangle, Washington, scale 1:24,000, Open File Map 80-2013, U.S. Geol. Surv., Reston, Va., 1980.

Molenaar, D., and J. B. Noble, Geology and related ground-water occurrence in southeastern Mason Co., Washington, Water Supply Bull.Wash. Dep. Water Resour., 29, 145 pp.,1970.

Noble, J. B., and E. F. Wallace, Geology and groundwater resources of Thurston Co., WA, vol. 2, Water Supply Bull. Wash. Dep. Water Resour., 10, 141 pp., 1966.

Nye, J. F., Theory of Regelation, Phil. Mag., 8(16), 1249-1266, 1968.

Nye, J. F., A calculation on the sliding of ice over a wavy surface using a Newtonian viscous approximation, Proc. R. Soc. London, Ser. A, 311, 445-467, 1969.

Nye, J. F., Glacier sliding without cavitation in a linear viscous approximation, Proc. R. Soc. London, Ser. A, 315, 381-403, 1970.

Olmsted, T. L., Geological aspects and engineering properties of glacial till in the Puget Sound Lowland, Washington, in Proceedings of the 7th Annual Engineering Geology and Soils Engineering Symposium, University of Idaho, Moscow, Idaho, pp. 223-233, 1969.

Palmer, A. C., D. J. Goodman, M. F. Ashby, A. G. Evans, J. W. Hutchinson, and A.R.S. Ponter, Fracture and its role in determining ice forces on offshore structures, Ann. Glaciol., 4, 216-221, 1983.

Paterson, W. S. B., The Physics of Glaciers, 380 pp., Pergamon, New York, 1969.

Porter, S. C., Present and past glaciation threshold in the Cascade Range, Washington, U.S.A.: Topographic and climatic controls, and paleoclimatic implications, J. Glaciol., 18(78), 101-116, 1977.

Porter, S. C., K. L. Pierce, and T. D. Hamilton, Late Wisconsin mountain glaciation in the western United States, in Late Quaternary Environments of the United States, edited by H. E. Wright and S. C. Porter, pp. 77-111, University of Minnesota Press, Minneapolis, 1983.

Shaw, J., Genesis of the Sveg tills and Rogen moraines of central Sweden: A model of basal melt-out, Boreas, 8, 409-415, 1979.

Shoemaker, E. M., Subglacial hydrology for an ice sheet resting on a deformable aquifer, J. Glaciol., 32(110), 20-30, 1986.

Shreve, R. L., Movement of water in glaciers, J. Glaciol., 11(62), 205-214, 1972.

Smalley, I. J., Conjectures, hypotheses, and theories of drumlin formation, J. Glaciol., 27(97), 503-505, 1981.

Sugden, D. E., and B. S. John, Glaciers and Landscape: A Geomorphological Approach, 375 pp., Edward Arnold, London, 1976.

Terzaghi, K., Theoretical Soil Mechanics, 510 pp., John Wiley, New York, 1943.

Terzaghi, K., and R. B. Peck, Soil Mechanics in Engineering Practice, 2nd edition, 729 pp., John Wiley, New York, 1967.

Thorson, R. M., Ice-sheet glaciation of the Puget Lowland, WA during the Vashon Stade (Late Pleistocene), Quat. Res., 13, 303-321, 1980.

Tsukada, M., S. Sugita, and D. M. Hibbert, Paleo-ecology of the Pacific, I, Late Quaternary vegetation and climate, Verh. Internat. Ver. Limnol., 21, 730-737, 1981.

Turcotte, D. L., and G. Schubert, Geodynamics, 450 pp., John Wiley, New York, 1982.

Walder, J. S., Stability of sheet flow of water beneath temperate glaciers and implications for glacier surging, J. Glaciol., 28(99), 273-293, 1982.

Waldron, H. H., B. A. Liesch, D. R. Mullineaux, and D. R. Crandell, Preliminary geologic map of Seattle and vicinity, Washington, scale 1:31, 680, U.S. Geol. Surv. Geol. Invest. Map, I-354, 1964.

Wallace, E. F. and D. Molenaar, Geology and groundwater resources of Thurston Co., vol. I, Water Supply Bull. Wash. Dep. Water Resour., 10, 254 pp., 1961.

Walters, K. L. and Kimmel, G. E. Groundwater occurrence and stratigraphy of unconsolidated deposits, central Pierce Co., Washington, Water Supply Bull. Wash. Dep. Water Resour., 22, 428 pp., 1968.

Washington Department. of Natural Resources, Division of Geology and Earth Resources, Geothermal Resources of Washington, Geol. Map GM-25, Olympia, 1981.

D. B. Booth and B. Hallet, Quaternary Research Center, AK-60, University of Washington, Seattle, WA 98195.

N. E. Brown, Department of Geological Sciences, AJ-20, University of Washington, Seattle, WA 98195.